scientific reports

Check for updates

OPEN

Biomechanical bite simulation in *Eucyon davisi* (Mammalia, Canidae) and comparison with extant Canids

Peri Emanuele[1], Bartolini-Lucenti Saverio[1,2], Tseng Z. Jack[3] & Rook Lorenzo[1,4]✉

Despite their ecological impact as predators, several aspects concerning canid palaeoecology remain poorly investigated. This is curious because their evolutionary history displays an intriguing variability in feeding-related adaptations, representing an attractive research topic. To explore this topic, we digitally simulated the bite of the medium-sized fossil canid *Eucyon davisi* (Late Miocene-Early Pliocene) using Finite Element Analysis (FEA). The aim of this study is the improvement of our knowledge on the feeding ecology of this basal Canini through the comparison of its reaction stress and bite efficiency with those obtained from a sample of extant Canidae. The cranial models were acquired through CT-scan, and the FE simulation was built using a series of trusses to reconstruct the muscles. We simulated a bilateral canine bite, a unilateral carnassial bite, and a unilateral bite at the M1. The stress patterns and the estimated bite forces across the three simulated load cases suggest for *E. davisi* a generalist ecology recalling the living jackal-like forms of the genus *Lupulella*. Likely its dietary range covered small vertebrates and non-meat food. Moreover, the FEA results highlight a role of the frontal sinuses in the mechanical behaviour of the cranium during a biting action.

Canidae Fischer, 1817 is a very successful terrestrial carnivoran family whose members are widespread all over the world and play an important role as mesocarnivorous (diet consisting of 50–70% vertebrate meat)- and hypercarnivorous (diet consisting of more than 70% vertebrate meat) predators in all the terrestrial environments[1]. Moreover, they have an intriguing palaeobiogeographical history, since they reached present day broad distribution in brief and relatively recent times (between 5.5 and 0.5 Ma)[2–4]. In addition, the family Canidae displays a wide spectrum of ecomorphotypes ranging from hypercarnivory [e.g. *Canis lupus* Linnæus, 1758, *Lycaon pictus* (Temminck, 1820)] to hypocarnivory [diet consisting of less than 50% vertebrate meat, e.g., *Chrysocyon brachyurus* (Illiger, 1815), *Lupulella adusta* (Sundevall, 1847), *Nyctereutes procyonoides* (Gray, 1834)][5–7], besides the fossil hyperspecialized durophagous Borophaginae Simpson, 1945[6,8]. This is even more surprising if we consider their plesiomorphic and conservative cranial and dental morphology[6,9]. Canids became specialised as meat consumers multiple times along their history from generalist forms[9–11], suggesting a complex and partially unresolved ecological history. Considering this intricacy and the present diversity of canids, the palaeoecological investigation at the base of the modern clades appears thus an insightful task to reconstruct the past of this important carnivore family.

To unravel this matter, several studies explored the morphology of teeth and snout of extant and fossil canids[7,12–15]; even the inner features of the cranium can provide useful clues about the palaeoecology and evolution of extinct forms[5,6,16,17]. For instance, Van Valkenburgh et al.[17] investigated the role and function of the respiratory turbinates in canids and felids. Furthermore, Frosali et al.[5] recently inferred the dietary preferences of the stem-Canini *Eucyon adoxus* (Martin, 1971) through an advanced comparative morphological and quantitative study of the frontal sinuses across the family Canidae. However, also the morphofuctional aspects of the skull can be crucial to understand the way of living of the more basal and enigmatic species. For this reason, in the last decade, the use of digital biomechanical analysis has become a widespread approach to simulate biological structures and investigate mechanical performance of extinct taxa. Among the several methods employed in computed biomechanics (e.g., multibody dynamics, computed fluid dynamics), the finite element analysis (FEA) appears as one of the most widely used thanks to its flexibility and the multiple type of data provided, such as (among others) stress, displacement and reaction forces[18]. Carnivorans (especially species displaying extreme morphologies) are the ideal subjects for this kind of studies, given the key role played by biting action in predation and the consequent mechanical response of the cranium. McHenry et al.[19] simulated

[1]Department of Earth Science, Paleo[Fab]Lab, University of Florence, Florence, Italy. [2]Institut Català de Paleontologia Miquel Crusafont (ICP-CERCA), Universitat Autònoma de Barcelona, Cerdanyola del Vallès, Spain. [3]Department of Integrative Biology, University of California, Berkeley, CA, USA. [4]Changes Foundation, Sapienza Università di Roma, Rome, Italy. ✉email: lorenzo.rook@unifi.it

the bite of *Smilodon fatalis* (Leidy, 1868) and that of a modern lion [*Panthera leo* (Linnaeus, 1758)] to assess the biomechanical performance of the American sabre-toothed and reconstruct its predation strategy. On a similar trail, FEA was employed to compare the bite mechanics of *S. fatalis* with those of *Barburofelis fricki* Schultz et al., 1970 and *Thylacosmilus atrox* Riggs, 1933 to explore the ecology of diverse sabretooth species[20–22]. Tseng et al.[23–25] employed FEA to explore the skull adaptation to the durophagy and its evolutive history across Hyaenidae simulating the bite of *Chasmaporthetes lunensis* Hay, 1921 and *Dinocrocuta gigantea* Schlosser 1903. Such a biomechanical methods were applied even on fossil Canidae; more specifically, Tseng and Wang[6] investigated the adaptation to durophagy in *Borophagus* Cope, 1892 and *Epicyon* Leidy, 1858 simulating their bite using the finite element method and comparing them with other canids.

In this study, we used the FEA to simulate the bite of *Eucyon davisi* (Merriam, 1911) (Upper Miocene – Lower Pliocene), a medium-sized canid thought to be basal to the tribe Canini Fischer, 1817 and characterised by relatively flat frontals. The data from *E. davisi* were assessed against those acquired from a sample of modern canids, included here as living analogues. The main goal of this approach, applied for the first time on a basal Canini, was to explore the relationship between cranial architecture and diet in *E. davisi* through the evaluation of the bite-generated stress patterns and estimation of the bite efficiency. By means of this work, we were also interested in verifying the role of the frontal sinuses in the dealing of the cranial stress generated from a biting action. Indeed, one of the commonly accepted hypotheses regarding the function of these cavities, observed in many carnivorans, is related with the dissipation of stresses associated to the processing of prey items[26,27]. The outcomes of the analyses performed here shed new light on the feeding habits of *E. davisi*, refining our knowledge about the paleoecology of this enigmatic canid, and contributes to our understanding of the link between form and function across Canidae.

Results

The von Mises stress (see Materials and Methods for the definition) distribution obtained from the bite simulations in the canid species included in this study are reported in Fig. 1. In all the bite simulations, the zygomatic arch seems to be the most stressed region of the cranium with two particularly high peak areas (between 22 and more than 30 MPa) at its mid-length and at the base of the zygomatic process of the temporal bone.

In the canine bite simulation of *Eucyon davisi* we can observe a generally moderate level of stress (values between 5 and 15 MPa) affecting most of the snout (except for the most anterior portion), the pterygoid, the temporal in its ventrolateral portion, and the frontal in its lateral portion and only partially in dorsal view. Dorsally, two areas of higher stress (green/yellow in Fig. 1a) can be detected: one located between the infraorbital foramina (14.5 MPa) and one slightly more evident affecting the rostroventral margin of the orbit (peak values between 16.2 and 20.9 MPa). At level of the dorsal surface of the frontals, there are two symmetrical arc-shaped regions of low stress, and posteriorly the values rapidly decrease. Observing the von Mises stress in the bite simulations at the carnassial and M1, the resulting distribution patterns appear as clearly asymmetric. The carnassial bite simulation (Fig. 1b) of *E. davisi* displays the widest pattern of the von Mises stress involving the base of the snout, the lateral wall of the orbit and the dorsal surface of the frontal. Excluding the peaks registered on the zygomatic arch, the von Mises stress values are mostly between 4 and 16 MPa and the distribution pattern appears as quite homogeneous. A more stressed region (between 12 and 16 MPa) is located above the carnassial tooth where the fixed nodal constraint was placed. Such an area extends from the level of the P3 to the rostral end of the orbit. Even in this bite scenario, the rostroventral margin or the orbit exhibits relatively high stress values reaching values between 16.8 and 21.1 MPa. Since the fixed constraint was not greatly shifted from the carnassial bite simulation to the M1 bite simulation, the von Mises stress distribution in the latter is morphologically close to those seen at the carnassial tooth, and the regions under stress are grossly the same (Fig. 1c). However, in this last load case, the area including the lateral surface of the frontal and the alisphenoid is more stressed than in the carnassial bite simulation, with values ranging from 10.4 to 18.6 MPa and local peaks reaching 22 MPa immediately above the M1. Another peak can be seen again at the rostroventral margin of the orbit. Remarkably, this region displays high von Mises stress values in all the three simulations of the *E. davisi* specimen included in this study. Consequently, the rostroventral margin of the orbit may represent a common point of deformation caused by the force exerted by the masseter muscle group along with the reaction force produced by the fixed constraints simulating the prey item. Generally, the stress pattern in the M1 simulation appears as less homogeneous than in the former simulation due to a low-stress region located on the surface of the snout at level of the orbits.

Comparing the stress maps scaled by the F_i/A_c ratio in the canine bite simulations (Fig. 2), the resulting pattern in *E. davisi* appears as intermediate between *Lupulella mesomelas* (Schreber, 1775) and *L. adusta* both in term of intensity and extension of the peaks. Indeed *E. davisi* displays a particularly stressed area (green in Fig. 2a) on the dorsal surface of the snout at level of the nasofrontal suture. Such a peak has been detected also in the tested specimens of the genus *Lupulella* Hilzheimer, 1906 (Fig. 2j, m), though in *L. mesomelas* this area is less evident and in *L. adusta* more visible. In the canine bite simulation of *E. davisi* and *Lupulella* this area of relatively high stress is surrounded by a wide portion of the cranium affected by a light blue area indicating lower stress. However, in *E. davisi* and *L. mesomelas* this pattern seems to moderately influence the dorsal surface of the frontals, while in *L. adusta* it appears severely affected. Observing the scaled von Mises stress values for the simulations of posterior bites, the resemblances between *E. davisi* and the extant *Lupulella* jackals still emerges, in reason of the similar stress distribution and values generated by the biting action. Observing the patterns in correspondence of the biting tooth and on the frontal region, a slightly greater resemblance with *L. adusta* can be tentatively discerned. The stress trend diagrams (Fig. 3) show more clearly the closeness of *E. davisi* and the genus *Lupulella* in term of mechanic performance. This is especially true for the diagrams of the canine and carnassial bite; in which the trend *E. davisi* closely follows *L. adusta* and *L. mesomelas*. Interestingly, in the canine and carnassial bite simulations, the stress values sampled on *E. davisi* are closer to *L. adusta* on the snout and

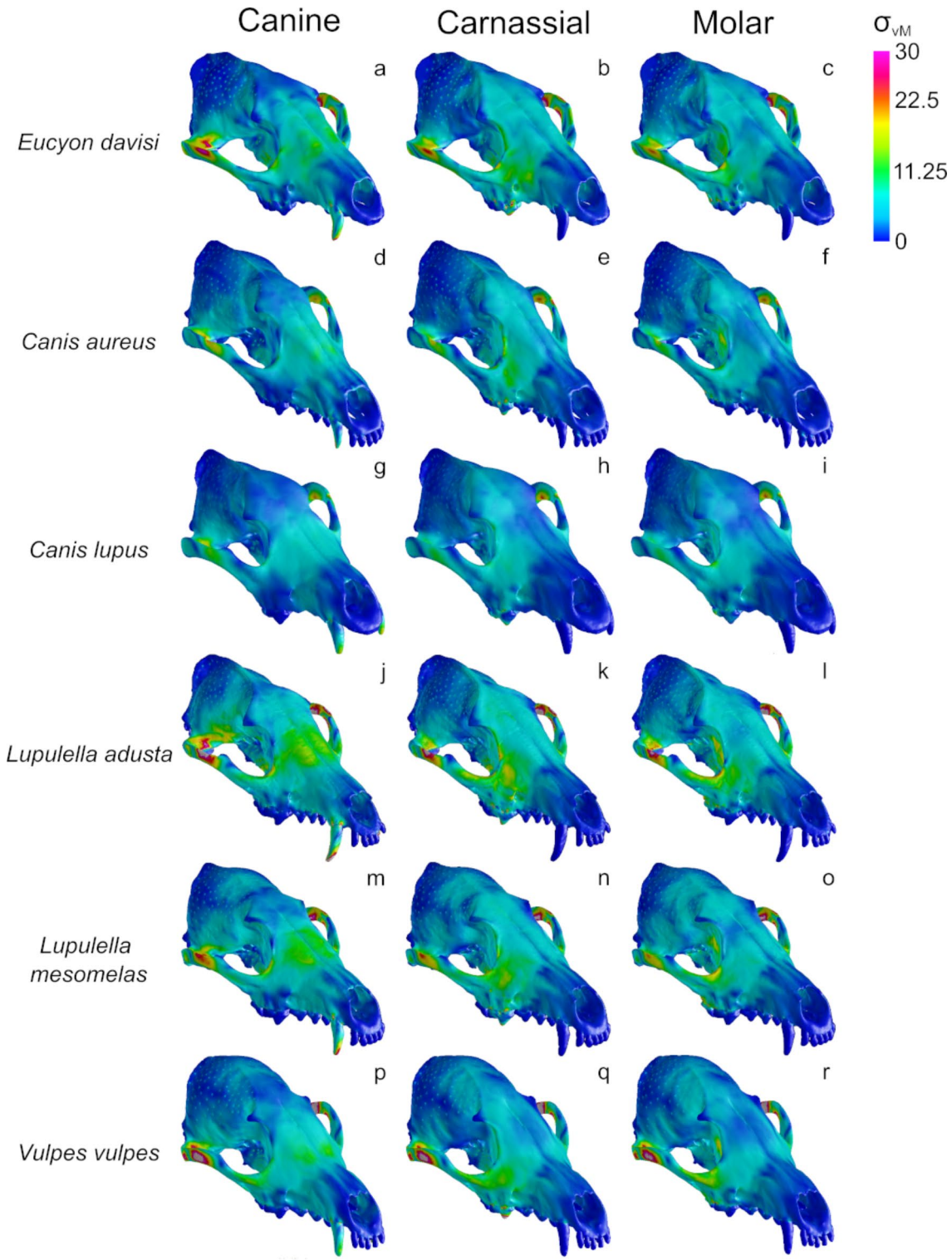

Fig. 1. Distribution maps of von Mises stress (σ_{vM}) resulting from the bite simulations at the canine teeth (**a**, **d**, **g**, **j**, **m**, **p**), carnassial (**b**, **e**, **h**, **k**, **n**, **q**) and M1 (**c**, **f**, **i**, **l**, **o**, **r**) on *Eucyon davisi* and the extant Canidae included in this study. The crania are in anterolateral view and not to scale. Note that the dotted pattern on the neurocranium are due to the punctiform force exerted by the trusses simulating the muscle fibres. Images created with the open-source software Inkscape v1.1 (The Inkscape Team) and GIMP v2.10.36 (The GIMP Development Team).

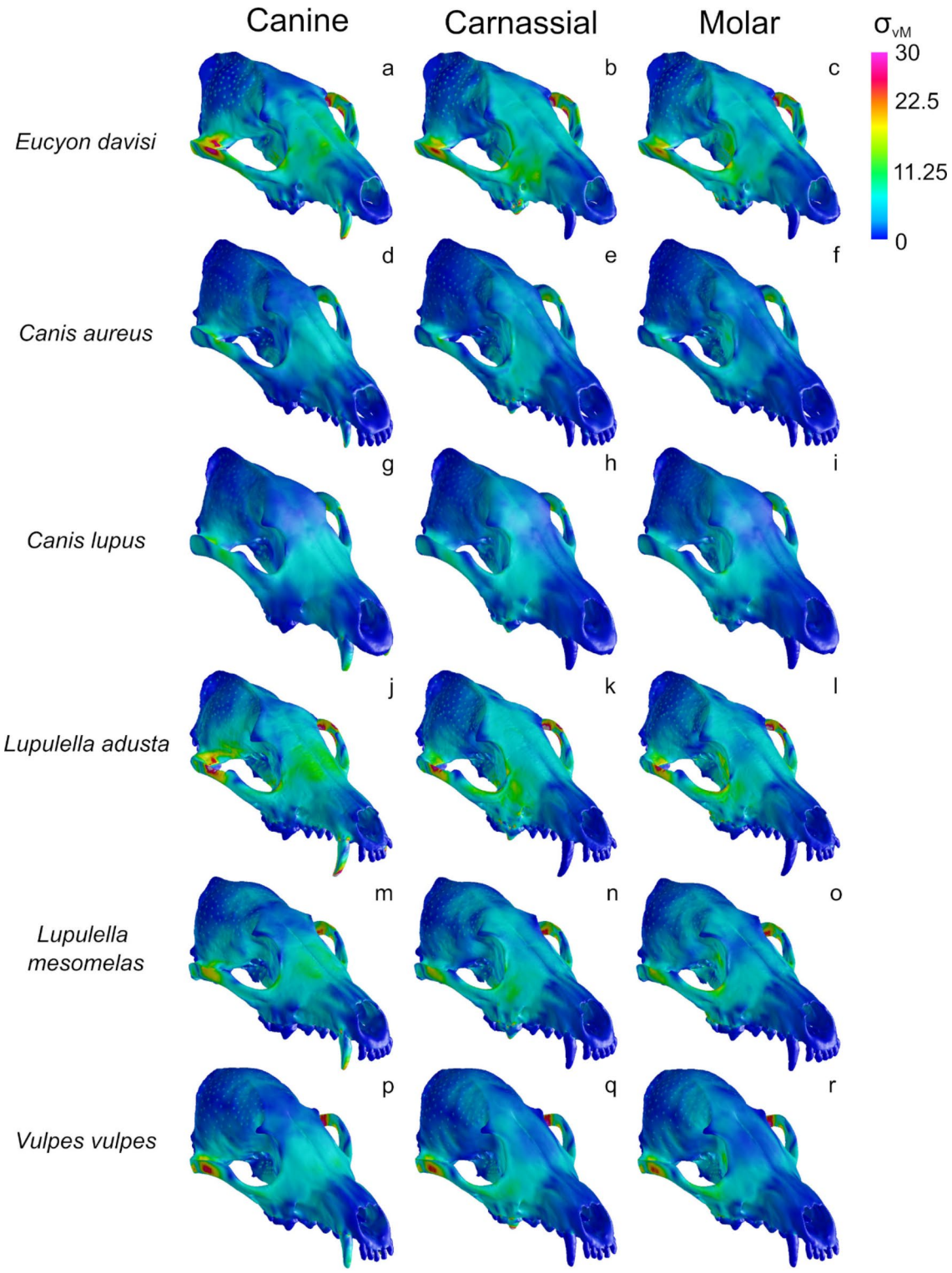

Fig. 2. Distribution map of von Mises stress (σ_{vM}) with the values scaled by the F_i/A_c ratio of *Eucyon davisi*. (**a**, **d**, **g**, **j**, **m**, **p**) bite simulations at the canine teeth, (**b**, **e**, **h**, **k**, **n**, **q**) bite simulations at the carnassial tooth, (**c**, **f**, **i**, **l**, **o**, **r**) bite simulations at the M1 tooth. The crania are in anterolateral view and not to scale. Note that the dotted pattern on the neurocranium of are due to the punctiform force exerted by the trusses simulating the muscle fibres. Images created with the open-source software Inkscape v1.1 (The Inkscape Team) and GIMP v2.10.36 (The GIMP Development Team).

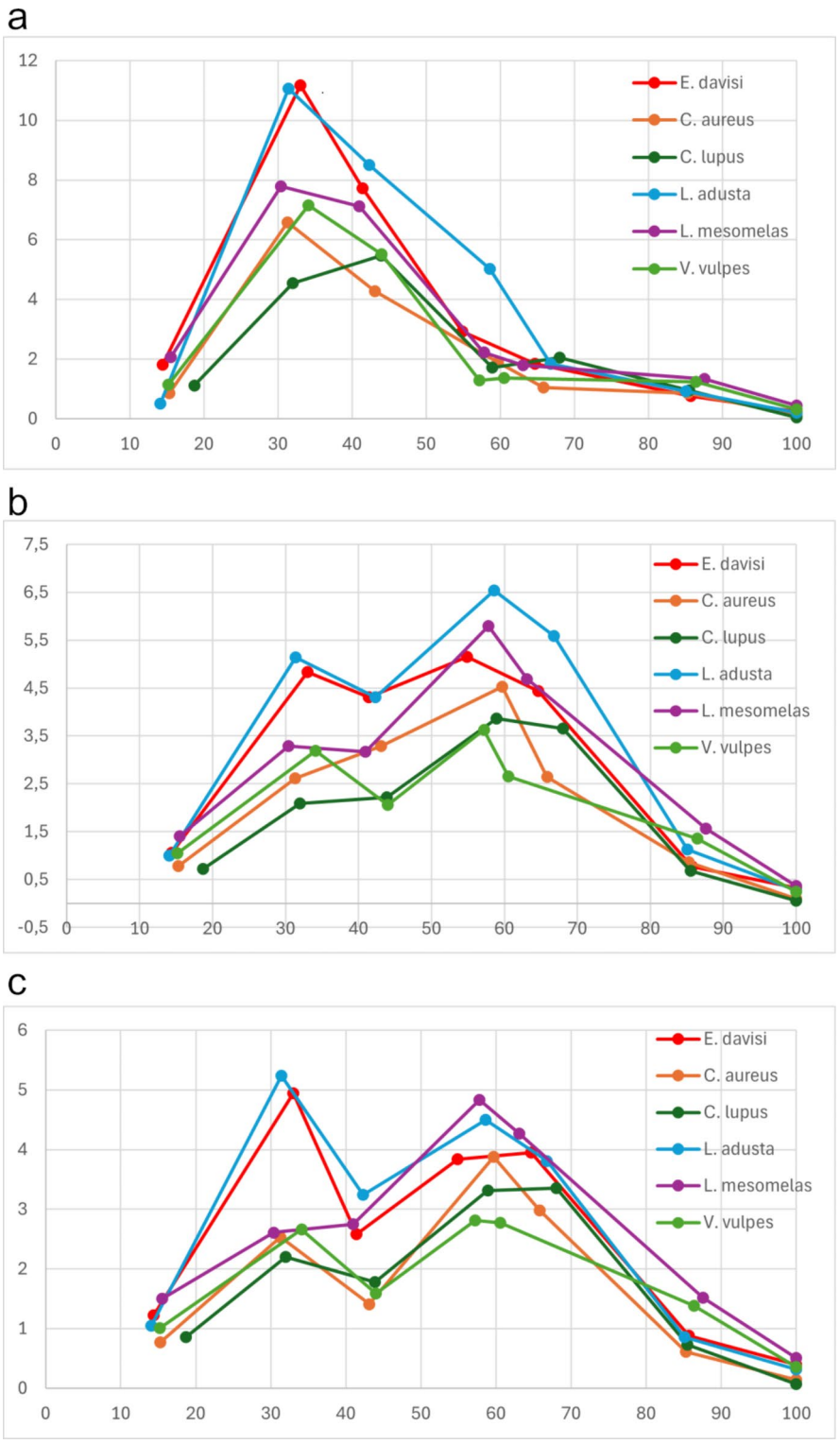

Fig. 3. Von Mises stress values (in MPa) scaled by the F_i/A_c ratio of *Eucyon davisi* sampled along a sagittal plane passing through the mid-point of the nasal width in the three bite scenarios. Results are shown for **a**, canine; **b**, carnassial; **c,** molar bite simulations. The analogous anatomical sampling points (nasal, rostrum at infraorbital foramina, rostrum at anterior border of orbits, frontal region between postorbital processes, frontal region at the postorbital constriction, centre of the parietal bone, and most posterior region of the dorsal cranium) are plotted as percentages of total skull length measured in dorsal view. Images created with the open-source software Inkscape v1.1 (The Inkscape Team).

	Temporalis force (*N*)	Masseter + pterygoid force (*N*)	Canine BF (*N*)	Carnassial BF (*N*)	M1 BF (*N*)	Bite efficiency (canine)	Bite efficiency (carnassial)	Bite efficiency (M1)
Eucyon davisi	319.2	408.12	121.63	361.85	446.68	0.0836	0.249	0.307
Canis aureus	209.34	289.53	86.76	266.96	331.3	0.087	0.268	0.332
Canis lupus	501.369	618.603	221.06	671.86	787.56	0.0987	0.3	0.352
Lupulella adusta	243.48	372.36	104.81	321.87	384.2	0.0851	0.261	0.312
Lupulella mesomelas	200.82	295.98	78.98	250.93	317.22	0.0795	0,252	0.319
Vulpes vulpes	149.1	213.48	60.9	178.35	219.58	0.084	0,246	0.303

Table 1. Input muscular data, resulting bite forces and bite efficiency values. *BF* bite force.

to *L. mesomelas* on the neurocranium. Notably, the sampling on the M1 bite simulation returned relatively low values for our specimen of *E. davisi* on the postorbital area with respect to those of *L. adusta* and *L. mesomelas*. Among the Canini considered here, *C. lupus* and *C. aureus* differs from *E. davisi* in displaying generally lower stress values in all the three load cases simulated here (Fig. 2d-i). Furthermore, in these two extant species, bite-related stress peaks affecting the splanchnocranium and/or on the rostral portion of the neurocranium are barely visible (*C. aureus*) or absent (*C. lupus*).

The bite efficiency values resulting from the FEA simulation are reported in Table 1. In general, the values are quite close among the canids tested here. However, *Canis lupus* shows slightly higher bite efficiency than the other taxa in all the simulated scenarios, suggesting that this species possesses the most effective structure in the transmission of the muscle force. Moreover, among the medium-sized species included in this study, *C. aureus* displays the highest bite efficiency. *Eucyon davisi* is placed in the lower part of the sample for its low bite efficiency values. The ratio values calculated for *E. davisi* are close to those of *Vulpes vulpes* (Linnaeus, 1758) in the bite simulations at the canine and M1, while it results closer to *L. mesomelas* in the carnassial bite simulations.

Discussion

Stress and paleoecology

The stress patterns observed on *Eucyon davisi* indicate that the cranium of this basal Canini was only moderately adapted to withstand the stress caused by a biting action. Specifically, in the bite simulations at the canines the snout is subjected to a quite evident stress peak at level of the infraorbital foramina (Figs. 1a and 2a), suggesting the presence of relatively high deformation in that region of the skull. Interestingly, observing the von Mises stress patterns scaled by the F_i/A_c ratio, we observed similar deformation peaks even in *Lupuella mesomelas* and *L. adusta* (Fig. 2j, m). Considering the scaled stress patterns, we can infer that *E. davisi* was not as adapted as *Canis lupus* and *C. aureus* Linnaeus, 1758 to use an anterior full power bite, as these two extant forms exhibit lower values of tensile stress (Fig. 2d-i) suggesting a stiffer cranial structure. Beside this, there are clear stress accumulation areas in correspondence to the biting teeth in the carnassial and M1 bite simulations (Figs. 1b and c and 2b and c,). The intensity of these peaks suggests that *E. davisi* was structurally less adapted to deal with the mechanical response related to posterior biting actions than other species considered in the present sample (e.g., *C. aureus* and *C. lupus*). In this feature, *E. davisi* resembles again *L. mesomelas* and *L. adusta*. Observing the data on the stress distribution and stress trend (Figs. 2 and 3), we can affirm that, among the examined living species, *L. adusta* and *L. mesomelas* exhibits the most similar structural behaviour to that of *E. davisi*. Interestingly, according to the ecological classification proposed by Van Valkenburgh and Koepfli[28], *L. mesomelas* is considered a mesocarnivorous form, while *L. adusta* exemplifies a hypocarnivorous ecomorphology. The prey range of *L. mesomelas* spans mainly from small vertebrates (e.g., rodents, birds, lagomorphs, reptiles), to occasional dietary inputs of larger mammals such as small antelopes[29–31]. The diet of *L. adusta* includes small vertebrates, insects, fruits, carrion, and plant material, and even scavenging represents an important food source for this jackal[30,31]. Based on the von Mises stress values (Fig. 1j-o), *L. mesomelas* seems having a generally stiffer cranial structure than *L. adusta*, and this is not surprising considering the greater elongation of the cranium in the latter. Consequently, the greater cranial strength of *L. mesomelas* may be interpreted as an adaptation to the hunt of medium-sized mammals such as small antelopes, a feeding habit absent in *L. adusta*[29–31]. The stress values resulting from the bite simulation of *E. davisi* are close (and often intermediate) to those of *L. adusta* and *L. mesomelas*. Following these results, we suggest for this basal Canini a generalist diet that likely included an input of non-meat food (i.e., insects and vegetal material). In consideration of the lower mechanic performance of *E. davisi* compared to that of *L. mesomelas*, it seems unlikely that the active hunt of medium- or larger-sized prey was a habit for this fossil canid, even if we cannot exclude this hypothesis. From an evolutionary perspective, the similarities in the mechanical behaviour between *E. davisi* and the genus *Lupulella* may be interpreted as evolutionary convergence or as the result of an ancestral morphology (symplesiomorphy). It should be noted that the genus *Lupulella* represents the most basal among the extant species considered here, and this seems to strengthen the second hypothesis. However, in our view, this does not invalidate the relationship between form and function in *E. davisi*, *L. adusta* and *L. mesomelas* highlighted by the FEA results.

Interestingly, the graphs showing the stress trends of the carnassial and M1 bite simulations display for *E. davisi* lower values at the sampling point 4 (between postorbital processes) and 5 (postorbital constriction) compared to those registered on the genus *Lupulella*, and placing the fossil form closer to *C. aureus* (Fig. 3b, c). This seems suggest a certain grade of stiffness of the postorbital region in the *E. davisi* specimen considered in this study (F: AM 97057), that could be due to a reinforcement of the postorbital portion of the frontals.

However, we cannot state if this feature has a functional value related to feeding or it is due to intraspecific variability. It is important to say that the cranium is a complex structure fulfilling to several functions[6]; thus, we decided to keep a cautious position in the interpretation of this specific cranial trait detected on F: AM 97,057, pending for additional specimens to be included in future investigations.

Bite reaction force and palaeoecology

Observing the raw data of the bite reaction force estimated on these studies, the extant species having the most similar magnitudes in values to those of *E. davisi* is *L. adusta*. Since the side-striped jackal is considered a generalist hypocarnivore[5,28], this apparently do not contrast with the von Mises stress results. However, the strength of the bite is highly influenced by the size of the cranium that determines the volume, and thus the input force, of the masticatory muscles. At this regard, among our sample, *L. adusta* has the closest measure of total cranial length to *E. davisi*, which can explain these results. Considering this, the sole data on the bite reaction force probably are not sufficient, although they are encouraging, to provide insights about the ecology in Canidae. The data on bite efficiency provide additional information. According to our results, *E. davisi* exhibits one of the less efficient cranial structures in the transmission of the muscle force, close to *L. mesomelas* and *V. vulpes*. These two extant Canidae are known to be highly generalist mesocarnivores[1,30,31], and this is in agreement with our conclusions from the von Mises stress analysis. Coupling the bite efficiency and stress data we can hypothesise for *E. davisi* a generalist predator paleoecology with a diet mainly based on small prey items (e.g., small mammals and small-sized reptiles) and non-meat food. This hypothesis represents the more conservative one even considering the similarities of *E. davisi* with *L. adusta*, *L. mesomelas* and *V. vulpes* as well as the overlapping in the diets of meso- and hypocarnivores. Moreover, such an interpretation substantially concurs with previous analysis[14] based on morphometric parameters, in which *E. davisi* is interpreted as mesocarnivore.

Noteworthy, comparing the bite efficiency values obtained from the canids included in this study, we observe that there is not a clear separation between the mesocarnivore taxa and *L. adusta*, since this latter register very similar values to *L. mesomelas*, *C. aureus* and *V. vulpes*. This uncertainty may be explained by highly similar ecologies that do not generate an evident signal in the form-function link on the cranium. In other words, there may not be sufficient biomechanical demand to result in different FEA results between meso- and hypocarnivores. However, based on the data collected until now, we believe that using the sole bite efficiency it is hard to discern between mesocarnivore and hypocarnivore forms. Surely this kind of datum should be combined to evaluations of the mechanical performances as well as to morphological and morphometric parameters to draw reliable conclusions.

Biomechanical significance of the frontal sinuses

The function of the frontal sinuses in the tribe Canini has been a subject of debate, and the matter is still not fully resolved. A factor that complicates this research question is also the presence of phylogenetic signal in the morphology of these structures[5]. However, the link between frontal sinuses and diet in Canidae has been always clear and pointed out by several scholars[16,32–34]. In this study, we wanted also to assess the influence of the frontal sinuses in the dealing of the stress experienced by the cranium during a biting action.

Observing the von Mises stress patterns of the canine bite simulations (Fig. 2a, d, g, j, m), we observed a decrease of the values as well as a patchy distribution in correspondence of the frontal sinus areas in *C. aureus*, *C. lupus*, *E. davisi* and *L. mesomelas*. Among these, *C. lupus* and *C. aureus* are surely the species in which this effect is more evident. Within our sample, *C. lupus* bears the most developed, domed and complex frontal sinus ornamented with grooves created by inner bony struts[5]. In addition, the grey wolf is a hunter of large-sized mammals (hypercarnivorous group hunter following Van Valkenburgh and Koepfli[28]), and it is intuitive that the capture of such prey items requires a great use of the anterior bite and a robust cranium. At a first sight, this seems to support interpretations that link the developing of the frontal sinuses with the stress dispersion. In *L. adusta* almost no decrease of the stress values in the frontal region is visible in the canine bite simulation. This species, the only hypocarnivore in our sample, displays rostro-caudally elongated frontal sinuses with an almost flat rostro-lateral lobe[5]. This feature gives to the sinuses of *L. adusta* a unique flattened and obtuse-angled morphology that differs both from the hypercanivorous *C. lupus* and from the mesocarnivorous forms *C. aureus* and *L. mesomelas*. These species share with *E. davisi* a quite simple morphology without the evident development of sinus copmlexity observed in *C. lupus* and in general a lesser development compared to the latter[5]. Furthermore, *C. aureus*, *E. davisi* and *L. mesomelas* exhibits in lateral view a domed dorsal shape, recalling in this *C. lupus* although to a far lesser degree. Thus, considering the morphology of the frontal sinuses along with the stress distribution (Figs. 1 and 2), we believe that the arched morphology may represent a relevant factor in the dealing of the cranial reaction stress caused by a bite taken with canines. Indeed, such a dome of the frontal sinuses may work as a discharging structure to reduce the bite-related solicitations on the frontal bones. A separate discussion should be conducted for *V. vulpes* (Fig. 2p). Indeed, this member of the tribe Vulpini Hemprich and Ehrenberg 1832 lacks the frontal sinuses, and it has an ossified cranial vault with a few trabeculae and canals. The von Mises stress values at the level of the frontal bones are comparable to those observed in other Canidae provided of frontal sinuses (e.g., *L. mesomelas*, *C. aureus*), and this seems to contrast with our interpretation. However, the lack of these structures in *V. vulpes* can be outlined in the peculiar 'hourglass' shape of the pattern and in its uniformity. This unique combination of features may be due to the ossification of the cranial vault and the presence of the vulpine crease (a fold of the postorbital process typical of the tribe Vulpini). Another peculiarity of the cranium of *V. vulpes* is represented by a slight dorsal convexity of the bones between the orbits. It is possible that the ossified cranial vault and the convex infraorbital region compensate the lack of the frontal sinuses in a canine bite scenario[35].

Observing the results of the carnassial (Fig. 2b, e, h, k, n) and M1 (Fig. 2c, f, i, l, o) bite simulations, the influence of the frontal sinuses in the stress dealing is not fully clear across the tested sample. Indeed, in *E.*

davisi, *L. adusta* and *L. mesomelas* these cavities seem having little or no influence. On the other hand, *C. lupus* displays particularly low values of von Mises stress on the dorsal surface of the frontal and a characteristic striated pattern in the carnassial and molar bite simulations. We deem that these effects are due to the presence of bony struts projecting inside the frontal sinus cavities, which may act as reinforcements against the tensile stress and reduce the solicitations on the neurocranium during the processing of food items. Notably, such a supporting function of these frontal sinus structures also was proposed by other authors[36,37]. Furthermore, this agrees with the known ecology of the grey wolf, since this canid sometimes process even the bone of its prey[6]. Furthermore, we detected low stress values even on the frontals area of *C. aureus* (Fig. 2e, f) despite it having a similar ecology to the mesocarnivorous jackal *L. mesomelas*. Such a pattern likely is due to the shortened and robust cranial shape of *C. aureus*, and we cannot exclude that the morphology of its frontal sinuses may have an effect on mechanical performance. According to our results, *C. aureus* represents the most similar specimen to *C. lupus* for stress values and bite efficiency. In addition, the golden jackal is the phylogenetically closest species to the grey wolf and one of the most derived among the Canidae selected here. Therefore, the mechanical behaviour of the cranium, which depends on its morphology, is likely to be influenced not only by the ecology but also by phylogeny. The presence of a phylogenetic signal in the morphology of the frontal sinuses of the tribe Canini has been reported by Frosali et al.[5] and supports our interpretation here.

Based on results obtained from the Canini included in this work, it seems that the frontal sinuses are somewhat involved in dealing the stresses affecting the cranial vault generated by a biting action. The simulation performed in this work suggest that the frontal sinuses play an important role in the improvement of the cranial mechanical performance in an anterior bite load case. However, the results of the carnassial and M1 bite simulations are ambiguous. In *E. davisi* as well as in the genus *Lupulella* the frontal sinuses seem to have little influence in the response of the cranium during the cutting and mastication. But apparently this is not true for *C. aureus* and even less in *C. lupus*, even if they have quite different ecologies (mesocarnivore the first, hypercarnivore the latter). Interestingly, *V. vulpes* may exploit the dorsal convexity observed on its cranium to reduce the load in the cranial vault. This interpretation is supported by the low stress values displayed by this taxon on the dorsal portion of the cranium between the orbits.

The mechanical behaviour of a complex structure like the mammalian cranium is a wide and complicated research topic. Surely, besides to the inner structure, there are multiple factors that concur to determine the stress pattern experienced by the cranium of a predator during a biting action. As an example, even the elongation of the snout and the cranial proportion play an important role in the structural reaction to the bite-related stresses. This is evident in *L. adusta*, which appears as the species with the most stressed cranium among those included here, but it is also the form with the slenderest snout and elongated cranium. Despite this, from the present study, it is evident that in the tribe Canini the frontal sinuses perform a stress-relieving and redistribution function on the stress generated by a bite. Further bite simulations on other Canidae species, both extant and extinct, will shed new light on the matter and will improve our comprehension of the ecology and palaeoecology of this important family of terrestrial predators.

Materials and methods

Sample availability

This study focuses on the study of a *Eucyon davisi* cranium (F: AM 97057) from the Early-Late Pliocene of the Yushe Basin (Xiakou, China)[38], currently stored at the American Museum of Natural History of New York (U.S.A.).

The comparative analyses were performed using data derived from the following specimens as modern analogues of comparison:

- *Canis aureus* (CBL-298).
- *C. lupus* (MZUF-2032).
- *Lupulella adusta* (MZUF-8496).
- *L. mesomelas* (MZUF-1128).
- *Vulpes vulpes* (CBL-1015).

Eucyon davisi cranium (F: AM 97057) high resolution CT-scans were performed at the University of Texas X-ray CT facility by George Lyras (Athens), with permission to study the specimen from AMNH curators[39].

We included the species of Canini listed above in order to cover most of the dietary variability displayed by this clade (hypercarnivore, mesocarnivore and hypocarnivore). Besides these, we also considered *Vulpes vulpes* to assess the stress patterns in a representative of the tribe Vulpini since in this group the frontal sinuses are lacking (the sole exceptions are some species belonging to the genus *Nyctereutes* Temminck, 1838). All the 3D models of the specimens were acquired by CT-scan, and the crania were aligned with the respective dentition and mandibles in Blender. For a detailed description of the acquisition and processing of the models see the supplementary materials.

Data availability

The complete set of data generated and analysed during the current study are available from the corresponding author on reasonable request.

Muscle force Estimation

For the purposes of this study, we considered a condition of static bite, when the velocity of the mandible elevator muscles is 0 m/s, and the force exerted by them is isometric[40,41]. In such a condition, the force value produced by a muscle is equal to its anatomical cross-section area (CSA) multiplied by the specific muscular tension. In the

present study, we assumed a value of 30 N/cm^2 for the muscular tension, following what previously did in many other papers investigating the mammalian bite[20–22,42,43]. Such a value has been acknowledged as underestimated when applied to masticatory muscles of mammals; due to their highly pennated morphology and to variation in the fibre length[19,20,40,41]. However, considering the uncertainty about the muscular architecture of fossil carnivorans, we decided to employ this value in our analyses as a conservative estimation that provides a repeatable protocol and more comparative results[20]. The CSA of the mandible elevator muscles was estimated in Blender using the dry-skull method proposed by Thomason[42] as 'temporalis muscle CSA' and 'masseter + pterygoid muscle CSA'.

Finite element model

The 3D meshes of the cranium, dentition and mandibles aligned in Blender were exported as stl files and uploaded in STRAND7 (Strand7 Pty. Ltd., Sydney, Australia) for the building of the finite element model and the setting of the simulation. Strand7 imported the vertices and faces of the 3D meshes as nodes and plates respectively; after a cleaning operation, we used the tool "automesh from plates" to generate solid meshes composed by 4-noded tetrahedral elements having two different material properties (one for the bone tissue and one for teeth). The number of tetrahedral elements varied between 3,931,409 and1,499,024 for the cranium, and between 1,392,144 and 213,633 for teeth. We assigned to the two material properties values of elastic modulus and Poisson's ratio that was compatible with the mammalian bone and dentine (bone: E = 13.7 GPa, υ = 0.30; teeth: E = 38.6 GPa, υ = 0.4), following previously published procedures[20–22,44,45]. The teeth were connected with the cranium by means a series of coupled links placed both at level of the crown-root interface and on the root apices; such a kind of entities transmit the displacement and/or rotation from one node to another. We placed 5 links on the single-rooted teeth, 8 links on the double-rooted teeth and 9 on the triple-rooted teeth. As previously did in Tseng and Wang[6], temporomandibular joint was simulated fixing two nodes at the mandibular fossae (one for each side) by two constraints only allowing the rotation around the axis perpendicular at the sagittal plane. Similarly, we fixed in a similar way the mandible at the level of the mandibular condyles roughly in correspondence of the constraints on the cranium.

The mandible elevator muscles included here were the temporalis group, the masseter group and the pterygoid group, and their architecture was taken from Hermanson[46]. The muscles were simulated through pretensioned beam elements transmitting an axial compression, defined as trusses. The tension value assigned at every truss was calculated dividing the muscular force estimated with the dry-skull method by the number of trussed assigned to the relative muscle. In our bite simulations we used 260 trusses for the temporalis muscles, 102 trusses for the master muscles and 52 trusses for the pterygoid group, reaching a total of 414 trusses.

To simulate the resistance of the food item during a biting action we placed a series of fixed constraint at the tip of the teeth involved in the simulation. Indeed, varying the position and the number of the dental constraints allowed us to simulate the following bite scenarios:

- bilateral canine bite, two constraints at the tips of the C;
- unilateral carnassial bite, one constraint at the paracone of the P4;
- unilateral molar bite, one constraint at the protocone of the M1;

The reaction force measured the teeth constraints represent the bite force measured at that specific point following several published papers[40,41,47]. To evaluate the bite efficiency across the load scenarios simulated here, the ratio between the estimated bite forces and the total input muscle force was calculated, and the values were matched among the species. This parameter represents how much of the force produced by the masticatory muscles is expressed at the dentition and thus it evaluates the efficiency of the skull in transmitting the muscle energy. The stress produced in all the bite simulations has been expressed as values of von Mises stress, a combined measure of the major stresses affecting the models. Such a measurement method is widely accepted as a good estimator of the reaction of a body under ductile failure condition, as observed in cortical bones[6,48]. In order to remove the any possible scale effect due to differences of size among the included taxa we scaled the von Mises stress values on the surface area of the cranium (as the stress is proportional to area)[48]. We calculated the ratio between the total input force (F_i) and cranial surface area (A_c) among the taxa. Since *E. davisi* represents the focus of this study, we used this fossil canid as a reference comparing its F_i/A_c ratio with those of all the other taxa in the form of a secondary ratio $[(F_i/A_c)_{taxon}/ (F_i/A_c)_{Eucyon}]$. Then, we applied such a scaling factor to the von Mises stress values though the Combination function of Strand7 and visualised the stress distribution as colour patterns. Furthermore, we sampled the values of the von Mises stress on specific points of the cranium (nasal, rostrum at infraorbital foramina, rostrum at anterior border of orbits, frontal region between postorbital processes, frontal region at the postorbital constriction, centre of the parietal bone, and posterior region of the dorsal cranium) along a plane passing through the right nasal and frontal bone and plotted on a graph, following what done by Tseng and Wang[6]. Through the study of the von Mises stress values and distribution, we discussed the mechanical efficiency of the tested crania. Moreover, the comparison of the scaled von Mises stress patterns among the tested species allowed us to evaluate the paleoecology of *E. davisi* in relation to its morphological adaptation.

Data availability

The complete set of data generated and analysed during the current study are available from the corresponding author on reasonable request.

Received: 7 December 2024; Accepted: 25 March 2025
Published online: 16 July 2025

References

1. Castelló, J. R. *Canids of the World* (Princeton University Press, 2018).
2. Sotnikova, M. & Rook, L. Dispersal of the Canini (Mammalia, Canidae: Caninae) across Eurasia during the late miocene to early pleistocene. *Quat Int.* **212**, 86–97 (2010).
3. Tedford, R. H., Wang, X. & Taylor, B. E. Phylogenetic systematics of the North American fossil caninae (Carnivora: Canidae). *Bull. Am. Mus. Nat. Hist.* **2009**, 1–218 (2009).
4. Wang, X. & Tedford, R. How dogs came to run the world. *Nat. Hist.* **117**, 18–23 (2008).
5. Frosali, S. et al. First digital study of the frontal sinus of stem-Canini (Canidae, Carnivora): Evolutionary and ecological insights throughout advanced diagnostic in paleobiology. *Front. Ecol. Env*. https://doi.org/10.3389/fevo.2023.1173341 (2023).
6. Tseng, Z. J. & Wang, X. Cranial functional morphology of fossil dogs and adaptation for durophagy in *Borophagus* and *Epicyon* (Carnivora, Mammalia). *J. Morphol.* **271**, 1386–1398 (2010).
7. Wang, X., Tedford, R. H. & Antón, M. *Dogs: their Fossil Relatives and Evolutionary History* (Columbia University, 2008). https://doi.org/10.7312/wang13528
8. Wang, X., Tedford, R. H. & Taylor, B. E. Phylogenetic systematics of the borophaginae (Carnivora: Canidae). *Bull. Am. Mus. Nat. Hist.* **243**, 8–356 (1999).
9. Van Valkenburgh, B., Wang, X. & Damuth, J. Cope's rule, hypercarnivory, and extinction in North American Canids. *Science* **306**, 101–104 (2004).
10. Holliday, J. A. & Steppan, S. J. Evolution of hypercarnivory: the effect of specialization on morphological and taxonomic diversity. *Paleobiology* **30**, 108–128 (2004).
11. Van Valkenburgh, B. Iterative evolution of hypercarnivory in Canids (Mammalia: Carnivora): evolutionary Interactions Among Sympatric Predators. *Paleobiology* **17** (4), 340–362 (1991).
12. Van Valkenburgh, B., Sacco, T. & Wang, X. Pack hunting in miocene borophagine dogs: evidence from craniodental morphology and body size. *Bull. Am. Mus. Nat. Hist.* **279**, 147–162 (2003).
13. Meloro, C., Hudson, A. & Rook, L. Feeding habits of extant and fossil Canids as determined by their skull geometry. *J. Zool.* **295**, 178–188 (2015).
14. Bartolini-Lucenti, S. & Rook, L. *Canis' ferox* revisited: diet ecomorphology of some long gone (Late miocene and Pliocene) fossil dogs. *J. Mamm. Evol.* **28**, 285–306 (2021).
15. Meloro, C. & Sansalone, G. Palaeoecological significance of the Wolf event as revealed by skull ecometrics of the canid guilds. *Quat Sci. Rev.* **281**, 107419 (2022).
16. Curtis, A. A. & Van Valkenburgh, B. Beyond the sniffer: frontal sinuses in carnivora. *Anat. Rec.* **297**, 2047–2064 (2014).
17. Van Valkenburgh, B., Theodor, J., Friscia, A., Pollack, A. & Rowe, T. Respiratory turbinates of Canids and felids: a quantitative comparison. *J. Zool.* **264**, 281–293 (2004).
18. Rayfield, E. J. Finite element analysis and Understanding the biomechanics and evolution of living and fossil organisms. *Ann. Rev. Earth Pl Sc.* **35**, 541–576 (2007).
19. McHenry, C. R., Wroe, S., Clausen, P. D., Moreno, K. & Cunningham, E. Supermodeled Sabercat, predatory behavior in Smilodon fatalis revealed by high-resolution 3D computer simulation. *Proc. Natl. Acad. Ssci U S A.* **104**, 16010–16015 (2007).
20. Figueirido, B., Lautenschlager, S., Pérez-Ramos, A. & Valkenburgh, B. V. Distinct predatory behaviors in Scimitar- and Dirk-Toothed Sabertooth cats. *Curr. Biol.* **28**, 3260–3266e3 (2018).
21. Figueirido, B., Tucker, S. & Lautenschlager, S. Comparing cranial biomechanics between *Barbourofelis Fricki* and *Smilodon fatalis*: is there a universal killing-bite among saber-toothed predators? *Anat. Rec*. https://doi.org/10.1002/ar.25451 (2024).
22. Janis, C. M., Figueirido, B., DeSantis, L. & Lautenschlager, S. An eye for a tooth: *Thylacosmilus* was not a marsupial saber-tooth predator. *PeerJ* **8**, e9346 (2020).
23. Tseng, Z. J. Cranial function in a late miocene *Dinocrocuta gigantea* (Mammalia: Carnivora) revealed by comparative finite element analysis. *Biol. J. Linn. Soc. Lond.* **96**, 51–67 (2009).
24. Tseng, Z. J. & Binder, W. J. Mandibular biomechanics of *Crocuta crocuta*, *Canis lupus*, and the late miocene *Dinocrocuta gigantea* (Carnivora, Mammalia). *Zool. J. Linn. Soc. Lond.* **158**, 683–696 (2010).
25. Tseng, Z. J., Antón, M. & Salesa, M. J. The evolution of the bone-cracking model in carnivorans: cranial functional morphology of the Plio-Pleistocene cursorial hyaenid *Chasmaporthetes lunensis* (Mammalia: Carnivora). *Paleobiology* **37**, 140–156 (2011).
26. Werdelin, L. Constraint and adaptation in the bone-cracking canid osteoborus (Mammalia: Canidae). *Paleobiology* **15**, 387–401 (1989).
27. Joeckel, R. M. Unique frontal sinuses in fossil and living hyaenidae (Mammalia, Carnivora): description and interpretation. *J. Vertebr Paleontol.* **18**, 627–639 (1998).
28. Van Valkenburgh, B. & Koepfli, K-P. Cranial and dental adaptations to predation in Canids. *Symp. Zool. Soc. Lond.* **65**, 15–37 (1993).
29. Colby, C. B. *Wild Dogs* (Duell, Sloan and Pearce, 1965).
30. Brain, C. K., Skinner, J. D., Chimimba, C. T., Smithers, R. H. & N. *The Mammals of the Southern African Subregion* (Cambridge University Press, 2005).
31. Nowak, R. M. *Walker's Carnivores of the World* (John Hopkins University, 2005).
32. Tedford, R. H., Taylor, B. E. & Wang, X. Phylogeny of the caninae (Carnivora: Canidae): the living taxa. *Am. Mus. Novit.* **3146**, 1–40 (1995).
33. Curtis, A. A., Orke, M., Tetradis, S. & Van Valkenburgh, B. Diet-related differences in craniodental morphology between captive-reared and wild Coyotes, *Canis latrans* (Carnivora: Canidae). *Biol. J. Linn. Soc. Lond.* **123**, 677–693 (2018).
34. Ruiz, J. V., Ferreira, G. S., Lautenschlager, S., de Castro, M. C. & Montefeltro, F. C. Different, but the same: inferring the hunting behaviour of the hypercarnivorous Bush dog (*Speothos venaticus*) through finite element analysis. *J. Anat.* **242**, 553–567 (2023).
35. Tanner, J. B., Dumont, E. R., Sakai, S. T., Lundrigan, B. L. & Holekamp, K. E. Of arcs and vaults: the biomechanics of bone-cracking in spotted hyenas (*Crocuta crocuta*). *Biol. J. Linn. Soc. Lond.* **95**, 246–255 (2008).
36. Witmer, L. M. The evolution of the antorbital cavity of archosaurs: A study in Soft-Tissue reconstruction in the fossil record with an analysis of the function of pneumaticity. *J. Vertebr Paleontol.* **17**, 1–76 (1997).
37. Siliceo, G., Salesa, M. J., Antón, M., Pastor, J. F. & Morales, J. Comparative anatomy of the frontal sinuses in the primitive sabre-toothed felid *Promegantereon ogygia* (Felidae, Machairodontinae) and similarly sized extant felines. *Estud Geol.* **67**, 277–290 (2011).
38. Tedford, R. H. & Qiu, Z. A new canid genus from the pliocene of Yushe, Shanxi Province. *Vert PalAsiat.* **34**, 27–40 (1996).
39. Lyras, G. A. The evolution of the brain in Canidae (Mammalia: Carnivora). *Scr. Geol.* **139**, 1–93 (2009).
40. Snively, E., Fahlke, J. M. & Welsh, R. C. Bone-Breaking bite force of *Basilosaurus Isis* (Mammalia, Cetacea) from the late eocene of Egypt estimated by finite element analysis. *PLoS One*. **10**, e0118380 (2015).
41. Peri, E., Falkingham, P. L., Collareta, A. & Bianucci, G. Biting in the miocene seas: Estimation of the bite force of the macroraptorial sperm Whale *Zygophyseter varolai* using finite element analysis. *Hist. Biol.* **34**, 1916–1927 (2022).
42. Thomason, J. J. Cranial strength in relation to estimated biting forces in some mammals. *Can. J. Zool.* **69**, 2326–2333 (1991).
43. Wroe, S., Colin, M. & Jeffrey, T. Bite club: comparative bite force in big biting mammals and the prediction of predatory behaviour in fossil taxa. *Proc. Roy. Soc. B-Biol. Sci.* 272, 619–625 (2005).
44. Slater, G. J., Dumont, E. R. & Van Valkenburgh, B. Implications of predatory specialization for cranial form and function in Canids. *J. Zool.* **278**, 181–188 (2009).

45. Slater, G. J. & Van Valkenburgh, B. Allometry and performance: the evolution of skull form and function in felids. *J. Evol. Biol.* **22**, 2278–2287 (2009).
46. Hermanson, J. W. The muscular system. in Miller's Anatomy of the Dog (ed Evans, H. E.) 185–280 (Elsevier Health Sciences, (2012).
47. Bourke, J., Wroe, S., Moreno, K., McHenry, C. & Clausen, P. Effects of gape and tooth position on bite force and skull stress in the Dingo (*Canis lupus Dingo*) using a 3-dimensional finite element approach. *PLoS One*. **3**, e2200 (2008).
48. Dumont, E. R., Grosse, I. R. & Slater, G. J. Requirements for comparing the performance of finite element models of biological structures. *J. Theor. Biol.* **256**, 96–103 (2009).

Acknowledgements

The authors are thankful to the kindness of the curators who granted access to the specimens in their care and provided permission to use CT data of the specimens or to access them online: Neil Duncan, Collections Manager of the American Museum of Natural History (New York, USA); George Lyras, National and Kapodistrian University of Athens (Athens, Greece); Fabio Di Vincenzo and Paolo Agnelli, former curators of, respectively, the Anthropological Museum and the Zoological Museum "La Specola", both part of the University of Florence Museum of Natural History (Florence, Italy). SBL thanks the support of CERCA Program, Generalitat de Catalunya.

Author contributions

E.P., S.B.-L., and L.R. conceived the paper. S.B.-L. digitized the specimens. E.P. performed the analyses and prepared the figures. The main text was prepared by E.P. with important contributions of S.B.-L., L.R. and J.T. who reviewed the manuscript including comments and improving significantly the first draft.

Declarations

Competing interests

The authors declare no competing interests.

Additional information

Supplementary Information The online version contains supplementary material available at https://doi.org/10.1038/s41598-025-95939-2.

Correspondence and requests for materials should be addressed to R.L.

Reprints and permissions information is available at www.nature.com/reprints.

Publisher's note Springer Nature remains neutral with regard to jurisdictional claims in published maps and institutional affiliations.